

## Steady-State Transport of High-Current Beams in a Focused Channel

I. Haber

*Naval Research Laboratory, Washington, D. C. 20375*

and

A. W. Maschke

*Brookhaven National Laboratory, Upton, New York 11973*

(Received 15 September 1978)

By following the orbits of several thousand particles in their self-consistent space-charge fields, the evolution of an unstable Kapchinskij-Vladimirskij distribution is examined until saturation is reached. A distribution is formed which is stable on a scale of hundreds of quadrupole magnets.

The possibility of using a heavy-ion beam to ignite an inertially confined pellet to thermonuclear temperatures<sup>1</sup> has increased the importance of transporting high-current beams of charged particles. Though the required beam ignition power and energy can be achieved using relatively modest extensions of present technology, any instabilities in the beam being transported that occur as extrapolation is made to higher current represent a major barrier to be overcome.

Extensive analysis of the transverse behavior of a transported beam in the presence of space-charge effects has been conducted by numerically integrating the Kapchinskij-Vladimirskij (KV) envelope equations.<sup>2-4</sup> Both theoretical and numerical evidences have indicated that these solutions are unstable to several classes of perturbations.<sup>5-8</sup> Evidence is presented here, through the use of computer simulations, that these instabilities saturate and a steady state evolves in which the beam remains stable over a scale of hundreds of transport lenses.

Figure 1 shows the  $x-p_x$  and  $y-p_y$  phase space of a KV distribution. It is a property of this distribution that each of these projections, in addition

to the  $x-y$  and  $p_x-p_y$  projections, is an ellipse of uniform density. The beam is assumed long compared with its transverse dimensions so that the evolution is assumed paraxial and variations along the beam are neglected.

The numerical model moves in a reference frame along with the beam so that the lens forces are electrostatic. The full Vlasov equation is simulated by following the orbits of several thousand simulation particles in their self-consistent electric fields. The numerical algorithm is of the PPOWER<sup>9</sup> type optimized for a Texas Instruments ASC computer. Numerical tests have shown the results to be essentially independent of variations in numerical parameters such as time step, system resolution, boundary location, and number of particles when they are varied by factors of 2 from the conditions used. Good agreement<sup>10</sup> has also been obtained in comparing growth rate and eigenfunction characteristics to theory when only one unstable mode is present.

A thin-lens quadrupole transport system is assumed with a phase advance of  $90^\circ$  per doublet. The phase-space plot of Fig. 1 shows a sample of 2000 particles out of 16 000 in the run, with initial conditions corresponding to a matched system having enough space charge to bring the

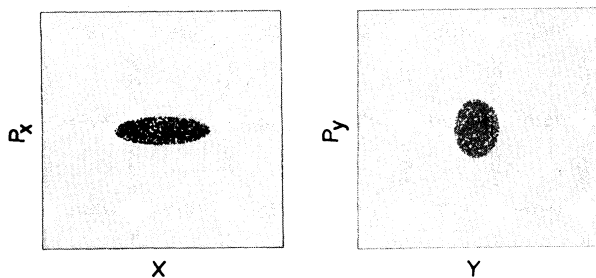


FIG. 1.  $x-p_x$  and  $y-p_y$  phase space of a Kapchinskij-Vladimirskij distribution with the  $90^\circ$  phase advance depressed by space charge to  $30^\circ$ . Two thousand sample particles are shown.

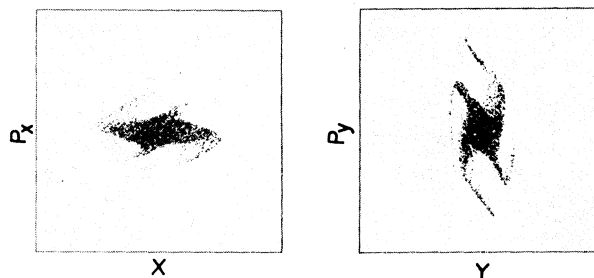


FIG. 2. Phase space of the distribution shown in Fig. 1 after passing through twenty doublets. The well-developed structure of the instability is apparent.

tune down to  $30^\circ$ . This system rapidly goes unstable and a complicated phase-space structure evolves as shown in Fig. 2, which shows the system phase space after twenty magnet pairs. After about forty magnet pairs, the system ceases to evolve significantly. Figure 3 shows the system phase space after 100 magnet pairs.

Figure 4 shows the evolution of the  $x$  and  $y$  emittances defined by the product of the root-mean-square values of  $x$  and  $p_x$  and  $y$  and  $p_y$ , respectively. This evolution displays the rapid growth of the instability and its subsequent saturation. The difference in the  $x$  and  $y$  behavior appears to be due to a combination of statistical effects and the systematic favoring of the  $x$  direction in the initial match because the initial conditions are chosen to minimize variation of the beam envelope between the first two  $x$ -focusing lenses. Once this anisotropy has developed, because of the lack of any dissipative mechanism for isotropization, it will persist.

The evolution of unstable eigenfunctions and the mechanisms which saturate their growth have been extensively studied in plasma physics.<sup>11</sup> In the present case, however, the complexity of the particle orbits in the combined focusing and space-charge fields has limited use of these concepts to explain the observed evolution of the rms emittance. Though much is known about the stability of KV systems,<sup>6</sup> the known unstable modes preserve the rms emittance. Growth and saturation of the emittance can therefore occur only after the initially small perturbation has grown enough to alter the KV equilibrium. By studying non-KV beams in a solenoidal channel Hofmann<sup>12</sup> has shown that deviation from the singular KV distribution stabilizes the beam. The periodic focusing structure in an alternate-gradient channel parametrically drives unstable modes which are not present in the uniform solenoidal channel and

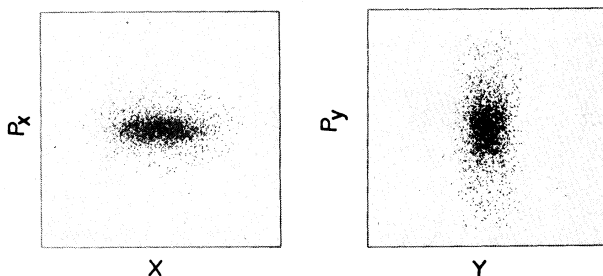


FIG. 3. Phase space after 100 doublets. Any evidence of the instability is no longer present.

little is known about non-KV distributions in alternate-gradient channels. However, the spreading of betatron frequencies which occurs as the system evolves away from the KV form can stabilize mode growth by introducing damping and also by reducing the number of particles in resonance with a particular mode.<sup>8</sup>

The behavior of a system which is not in equilibrium and where several unstable modes are nonlinearly interacting is difficult to predict in detail. For example, evolution of the distribution function which alters the range of betatron frequencies to stabilize one mode can destabilize another at a different resonance. Even if it were possible to predict the stabilization level of each mode this would not determine whether the distribution after stabilization is in equilibrium with the periodic focusing forces. At higher initial currents than shown here, numerical evidence does in fact suggest that an equilibrium is not achieved. Instead, the emittance continues to grow substantially for a time long compared with the apparent saturation time of the initially unstable modes. In the case being presented here a steady state is reached after only modest emittance growth and little particle diffusion in the physical channel. This behavior appears to depend on details of the nonlinear dynamics which are not yet understood.

A detailed characterization of the final distribution is beyond the scope of this communication. Though a plot such as  $f(p_x)$  at  $x=0$ , integrated over  $y$  and  $p_y$ , is somewhat Gaussian shaped, as are several other cross sections, the total picture may be somewhat more complex. For example, the ratio of rms to average absolute value of density in the  $x$  direction is 1.23. This is

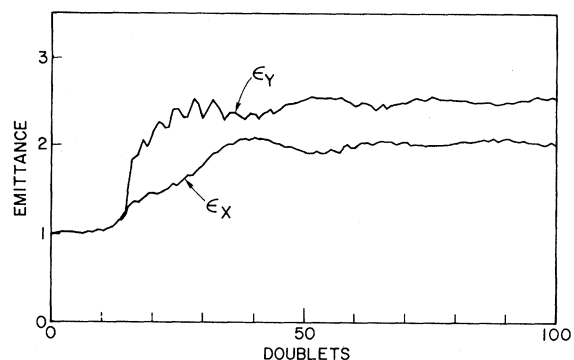


FIG. 4. Evolution of the  $x$ - $p_x$  and  $y$ - $p_y$  rms emittances showing the establishment of a steady state.

the same as the rms-to-average ratio in the  $y$  direction but different from both the  $p_x$  and  $p_y$  rms-to-average ratios, which are 1.33. The contour plot in Fig. 5 of the  $y$ - $p_y$  phase space at an  $x$ -focusing lens shows that the growth in emittance is mostly due to a spreading in the velocity of the distribution function and also shows a marked squaring from the elliptical contours of a KV distribution.

The simulations discussed were performed using normalized variables. To relate them to a physical transport system, the variables must be reconverted to physical units. The transport power in a quadrupole channel is then

$$P(W) = C(A/z)^{4/3} [B_q(T)]^{2/3} \times [\epsilon(\text{m rad})]^{2/3} (\beta\gamma)^{7/3} (\gamma - 1),$$

where  $P$  is the power,  $A$  and  $z$  are the mass number and charge state,  $B_q$  is the quadrupole pole tip field,  $\epsilon = 4\langle x^2 \rangle^{1/2} \langle x'^2 \rangle^{1/2}$  is the rms emittance, and  $x' = p_x/p_a$ .

The coefficient  $C$  is dependent on the distribution function in the beam, the aperture size, and the lens thickness. Since the thin lenses used in the simulation require an infinite pole-tip strength and are not physical, some assumption must be made as to lens thickness. Laslett<sup>13</sup> has shown that for a magnet system with half the space filled with magnets, with a  $90^\circ$  phase advance depressed to  $30^\circ$  by space charge, and with a KV distribution filling the aperture, the coefficient

corresponds to

$$C = 3.0 \times 10^{15}.$$

From this, an estimate of the coefficient corresponding to the distribution of Fig. 3 can be obtained. An aperture necessary to contain all the particles shown in Fig. 3 must be about twice as large as for the original KV distribution and so the pole-tip field must be correspondingly larger to maintain the same magnetic field gradient. This introduces a factor of  $2^{-2/3}$  leading to a coefficient of  $C = 1.9 \times 10^{15}$ . This is, however, in terms of the initial emittance. In terms of the final rms emittance, another  $2^{-2/3}$  is introduced giving a coefficient of  $C = 1.2 \times 10^{15}$ .

The coefficient represents the distribution shown in Fig. 5. A systematic search in parameter space may, in fact, show that much greater currents can be stably transported and that a proper choice of initial distribution will not lead to instability. The current result is, however, important because the power levels observed are consistent with those required for thermonuclear pellet ignition. Since the simulations include most of the important physics, these results seem to be a significant indication that transverse instabilities need not be a barrier to the use of heavy ion beams as a source of pellet ignition energy.

The authors wish to acknowledge the assistance and encouragement provided by Dr. J. P. Boris, Dr. T. F. Godlove, Dr. L. J. Laslett, and Dr. L. Smith. This work is supported by the U. S. Department of Energy.

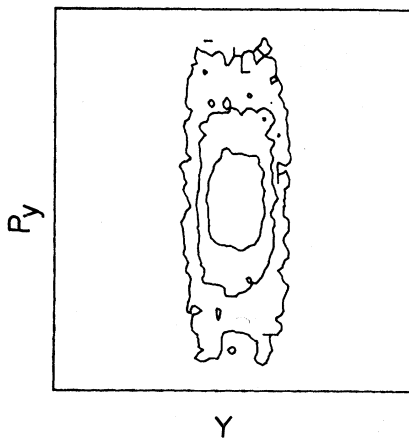


FIG. 5. Contour plot of the  $y$ - $p_y$  phase space shown in Fig. 3. Emittance growth is seen to be primarily due to spreading in velocity space and the contours are noticeably squared from the initial KV ellipses. Adjacent contours differ in density by a factor of 4.

<sup>1</sup>G. Kuswa, IEEE Trans. Nucl. Sci. 24, 975 (1977).

<sup>2</sup>I. M. Kapchinskij and V. V. Vladimírskij, in *Proceedings of the International Conference on High Energy Accelerator and Instrumentation*, edited by L. Kowarski (CERN, Geneva, 1959), p. 274.

<sup>3</sup>G. Lamberston, L. J. Laslett, and L. Smith, IEEE Trans. Nucl. Sci. 24, 993 (1977).

<sup>4</sup>T. K. Khoe and R. L. Martin, IEEE Trans. Nucl. Sci. 24, 1025 (1977).

<sup>5</sup>R. L. Gluckstern, in *Proceedings of the 1970 Proton Linear Accelerator Conference*, edited by M. R. Tracy (National Accelerator Laboratory, Batavia, Ill., 1970), Vol. 2, p. 811.

<sup>6</sup>S. Chattopadhyay, I. Hofmann, L. J. Laslett, and L. Smith, Lawrence Berkeley Laboratory, Reports No. Part I-HI-FAN 13, No. Part II-HI-FAN-14, and No. Part III-HI-FAN-15 (unpublished).

<sup>7</sup>P. M. Lapostolle, CERN, Geneva, Report No. CERN-

ISR/78-13, 1978 (unpublished).

<sup>8</sup>Ingo Hofmann, to be published.

<sup>9</sup>J. H. Orens, J. P. Boris, and I. Haber, in *Proceedings of the Fourth Conference on Numerical Simulation of Plasmas, Naval Research Laboratory, Washington, D. C., 1979*, edited by J. P. Boris and R. A. Shanny (Superintendent of Documents, Washington, D. C.,

1971).

<sup>10</sup>L. J. Laslett and L. Smith, to be published.

<sup>11</sup>Ronald C. Davidson, *Methods in Nonlinear Plasma Theory* (Academic, New York, 1972).

<sup>12</sup>Ingo Hofmann, to be published.

<sup>13</sup>L. J. Laslett, Lawrence Berkeley Laboratory, Berkeley, Report No. HI-FAN-11, 1977 (unpublished).

## Excess Ultrasonic Attenuation in $\text{As}_2\text{S}_3$ Glass after Electric Field Removal

T. N. Claytor<sup>(a)</sup> and R. J. Sladek

*Department of Physics, Purdue University, West Lafayette, Indiana 47907*

(Received 16 March 1979)

Increased ultrasonic attenuation is found in  $\text{As}_2\text{S}_3$  glass at 4.2 K after removal of a high electric field. The extra attenuation persists for a few minutes before disappearing, but can be reduced, or practically eliminated, by infrared radiation of moderate intensities. The effect is attributed to atomic relaxation accompanying electronic transitions in gap states where injected carriers have been trapped. The gap states may be valence-alternation pairs.

Microscopic understanding of the properties of disordered materials is still incomplete. Some of these properties, including the heat capacity,<sup>1,2</sup> thermal conductivity,<sup>1-3</sup> and the attenuation and velocity of ultrasonic waves,<sup>4-6</sup> exhibit behavior at low temperatures which has been explained in terms of tunneling in two-level systems<sup>7</sup> having various energy level separations and tunneling parameters. On the other hand, various electronic and optical properties of arsenic sulfide and selenide glasses, such as drift mobility, field effect, photoluminescence, and photoconductivity, have been explained in terms of the production, motion, and recombination of electron-hole pairs and the influence of localized states in the energy gap between valence and conduction bands.<sup>8</sup> The gap states have been associated with unfulfilled, or dangling, lone-pair bonds of the chalcogens which are occupied to various degrees so as to produce valence-alternation pairs<sup>9</sup> (VAP). In order to determine if there is a connection between the thermal-ultrasonic and electronic-optical phenomena, and thus between the two-level systems and the dangling-bond centers or VAP's, we have investigated the influence of high electric fields on the ultrasonic attenuation in  $\text{As}_2\text{S}_3$  glass.

Our attenuation measurements were made with the sample immersed in liquid helium at 4.2 K contained in a double Pyrex Dewar vessel. We employed a pulse-echo method in which the attenuation of pulses of 30-MHz longitudinal ultrasonic

waves was determined by averaging for 2.5 sec and recording the ratio of two echoes (usually 1 and 4) resulting from different numbers of round-trips in the sample. The minimum measurable change in attenuation amplitude was about 0.2%. We also applied dc voltages of up to 6 kV to the sample which was either in the dark or else in a beam of infrared (ir) radiation coming through a 1.0-mm-thick Ge filter in the path of light from a tungsten filament microscope lamp. The intensity of the ir radiation was measured with a Gen-Tec detector in place of the Dewar.

The samples were rectangular parallelepipeds of  $\text{As}_2\text{S}_3$  glass (about 1.5 cm  $\times$  1.5 cm  $\times$  0.5 cm) purchased from the American Optical Company. Most of the data reported herein were obtained on sample 8 of Ref. 5 which contains details about its characteristics. In addition, the sample surfaces were oxidized in air at 100°C for 3 h. Electrodes to which the high voltages were applied usually consisted of a 0.70-cm-diam spot of silver paint on the bottom of the sample and the coaxial chrome-gold plating on the bottom of the 0.635-cm-diam, X-cut, quartz transducer which was attached to the top of the sample with 4-methyl-pentene-1 to make the acoustic bond. However, in one case we used silver paint electrodes opposite one another on the side faces of the sample while the transducer was atop the sample, as before. Although this arrangement was plagued by dielectric breakdown to the sample holder, at voltages below breakdown it gave

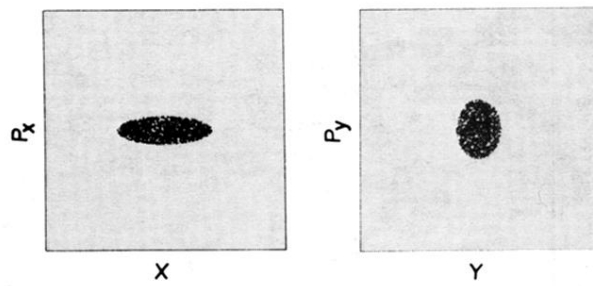


FIG. 1.  $x$ - $p_x$  and  $y$ - $p_y$  phase space of a Kapchinskij-Vladimirskij distribution with the  $90^\circ$  phase advance depressed by space charge to  $30^\circ$ . Two thousand sample particles are shown.

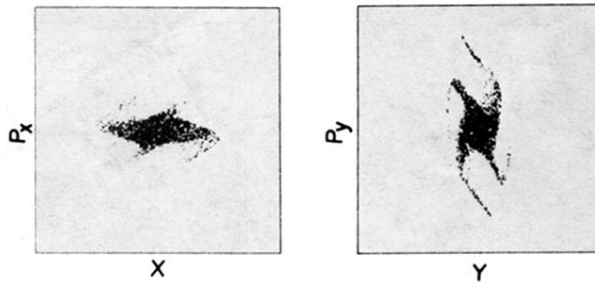


FIG. 2. Phase space of the distribution shown in Fig. 1 after passing through twenty doublets. The well-developed structure of the instability is apparent.

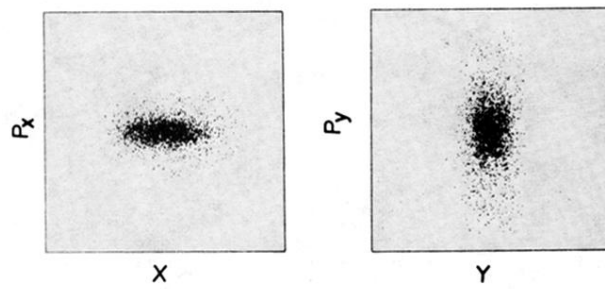


FIG. 3. Phase space after 100 doublets. Any evidence of the instability is no longer present.